

Towards Realistic Zero-Shot Classification via Self Structural Semantic Alignment

Sheng Zhang¹ Muzammal Naseer¹ Guangyi Chen^{1,2} Zhiqiang Shen¹
 Salman Khan^{1,3} Kun Zhang^{1,2} Fahad Khan^{1,4}

¹Mohamed bin Zayed University of AI ²Carnegie Mellon University

³Australian National University ⁴Linköping University

{firstname.lastname}@mbzuai.ac.ae

Abstract

Large-scale pre-trained Vision Language Models (VLMs) have proven effective for zero-shot classification. Despite the success, most traditional VLMs-based methods are restricted by the assumption of partial source supervision or ideal vocabularies, which rarely satisfy the open-world scenario. In this paper, we aim at a more challenging setting, *Realistic* Zero-Shot Classification, which assumes no annotation but instead a broad vocabulary. To address this challenge, we propose the Self Structural Semantic Alignment (S^3A) framework, which extracts the structural semantic information from unlabeled data while simultaneously self-learning. Our S^3A framework adopts a unique Cluster-Vote-Prompt-Realign (CVPR) algorithm, which iteratively groups unlabeled data to derive structural semantics for pseudo-supervision. Our CVPR process includes iterative clustering on images, voting within each cluster to identify initial class candidates from the vocabulary, generating discriminative prompts with large language models to discern confusing candidates, and realigning images and the vocabulary as structural semantic alignment. Finally, we propose to self-learn the CLIP image encoder with both individual and structural semantic alignment through a teacher-student learning strategy. Our comprehensive experiments across various generic and fine-grained benchmarks demonstrate that the S^3A method offers substantial improvements over existing VLMs-based approaches, achieving a more than 15% accuracy improvement over CLIP on average. Our codes, models, and prompts are publicly released at <https://github.com/sheng-eatamath/S3A>.

Introduction

In recent years, large-scale pre-trained Vision Language Models (VLMs) such as CLIP (Radford et al. 2021; Ren et al. 2022), ALIGN (Li et al. 2021), and BLIP (Li et al. 2022, 2023) have garnered significant attention for their remarkable zero-shot generalization ability on multifarious downstream tasks, particularly in recognizing unseen categories (Zhang et al. 2023). The common practice to leverage this ability is packing category names into a textual prompt (e.g., “A photo of a [CLS]”) and aligning image embeddings with text embeddings of filled prompts in VLM joint embedding space for classification. To adapt pre-trained VLMs to downstream unseen data, existing prevailing methods (Wu et al. 2023; Zang et al. 2022; Ghiasi et al. 2021) usually assume the access to source labeled data (e.g.,

in zero-shot learning (Zhou et al. 2022a; Gao et al. 2021)), target label distribution (e.g., in unsupervised prompt tuning (Kahana, Cohen, and Hoshen 2022)), or an *ideal vocabulary* that exactly matches the ground-truth label set or with very few open words (e.g., in open-vocabulary learning (Wu et al. 2023; Zang et al. 2022; Ghiasi et al. 2021)). However, this ideal vocabulary is unattainable without exhaustive annotation of all unseen data; whereas, human annotations are exorbitant and difficult to scale. Therefore, both assumptions are restrictive and impractical in open-world scenarios with diverse and dynamic nature.

In this paper, we embark on a journey towards *Realistic* Zero-Shot Classification (RZSC), a more challenging yet practical problem compared with conventional zero-shot learning due to its realistic conditions. Here, we term *Realistic* as the realistic nature of RZSC which aims to recognize categories on unseen datasets without annotation and ideal vocabulary, but with a vast, comprehensive vocabulary with more than 20K category names encompassing all common classes (Sariyildiz et al. 2021; Ridnik et al. 2021). However, it is challenging since the vast vocabulary can lead to alignment confusion among fine-grained options; as we witness the consistent and dramatic CLIP (Radford et al. 2021) performance drops and reduced neighborhood ranges in Fig. 1.

To confront this challenge, we introduce the Self Structural Semantic Alignment (S^3A) framework, which iteratively discovers structural semantic alignment from unlabeled data for joint self-learning. This is orchestrated through our unique Cluster-Vote-Prompt-Realign (CVPR) algorithm, a principled process comprising four key steps: (1) **Clustering** unearths inherent grouping structures within image embeddings, producing meaningful image semantics. (2) **Voting** associates each cluster with initial category candidates, representing potential pseudo-alignments. These two steps can be executed iteratively to obtain more reliable candidates. (3) **Prompting** leverages the power of large language models (LLMs) to discern nuanced candidates by augmenting prompts with discriminative attributes. (4) **Re-alignment** represents calibrating the cluster-vocabulary alignment with LLM-augmented prompts as pseudo structural semantic alignment labels. Incorporating our CVPR algorithm, our S^3A framework self-trains a student model based on extracted individual and structural semantic alignment labels from a stable teacher.

Setting	Vocab.	Annotation	Train
Zero-Shot Transfer	G.T.	✗	\mathcal{Y}_{tgt}
Zero-Shot Classification	G.T.	✓	\mathcal{Y}_{base}
Open-Vocabulary Learning	<2K	✓	\mathcal{Y}_{base}
Unsupervised Fine-tuning	G.T.	✗	\mathcal{Y}_{tgt}
RZSC	>20K	✗	\mathcal{Y}_{tgt}

Table 1: **Our realistic zero-shot classification and other related settings.** Here, following (Wu et al. 2023), we denote \mathcal{Y}_{base} and \mathcal{Y}_{tgt} as the sets of base training classes and target testing classes, which satisfies $\mathcal{Y}_{base} \cap \mathcal{Y}_{tgt} = \emptyset$. The shared learning goal of all settings is to recognize \mathcal{Y}_{tgt} in test data. Ground-truth is abbreviated as G.T.

Simultaneously, the teacher is updated by student weights to produce more reliable pseudo semantic alignments.

We extensively evaluate our **S³A** framework across multiple setups, spanning a variety of generic and fine-grained benchmarks. The results show that **S³A** not only consistently outperforms previous adapted State-of-The-Arts (SOTAs) under the RZSC setting on all benchmarks, but excels in out-of-vocabulary evaluation, where category names can fall outside the **S³A** vocabulary. It is worth noting the our **S³A** remarkably enhance naive CLIP by > 10% top-1 classification accuracy on average. Comprehensive evaluations evidence our **S³A** framework paves the way to this realistic challenging problem.

Our contributions include: (1) We propose a Self Structural Semantic Alignment (**S³A**) framework, to address the challenging *Realistic Zero-Shot Classification* problem, which jointly extracts and self-learns on the individual and structural semantic alignment. (2) We propose a Cluster-Vote-Prompt-Realign algorithm to reliably derive reliable structural semantic alignments between images and the large vocabulary. (3) **S³A** achieves SOTA performance on various generic and fine-grained benchmarks, remarkably boosting CLIP by over 10% accuracy, and even in the out-of-vocabulary scenarios.

Related Work

Zero-Shot Learning/Open-Vocabulary Learning with VLMs. Traditional (*Generalized*) *Zero-Shot Classification* (ZSC) aims to categorize novel classes in unseen test data with training on annotated base/seen classes with or without unlabeled target novel classes (Wang et al. 2019; Pourpanah et al. 2022). However, they usually assume auxiliary semantic information of both seen and unseen classes, *e.g.*, category attributes (Lampert, Nickisch, and Harmeling 2009), knowledge graph (Akata et al. 2015), textual keywords (Lei Ba et al. 2015; Cappallo, Mensink, and Snoek 2016). Recently, large-scale pre-trained VLMs have been introduced to alleviate these assumptions (Jia et al. 2021; Radford et al. 2021; Zhang et al. 2023). Furthermore, *Open-Vocabulary Learning* (OVL) (Wu et al. 2023; Zhou et al. 2023; Zhou, Loy, and Dai 2022; Karazija et al. 2023) are presented, which train the models on some annotated data (base

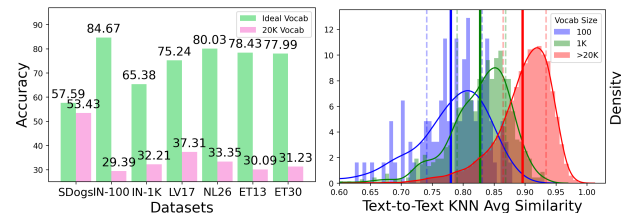


Figure 1: (a) Performance comparison between CLIP w/ an ideal vocabulary (Green) and w/ a large vocabulary of 20K categories (Pink). (b) Distribution plot of text-to-text average 3-Nearest Neighbors cosine similarity of each text embedding for three types of vocabulary: with ImageNet-100, ImageNet-1K, and 20K category names.

classes (Xu et al. 2023) or large-scale image-text pairs (Shin, Albanie, and Xie 2023)) and test them on open novel classes. Our RZSC setting differs from conventional ZSC and OVL in not requiring any labeled training data, and not assuming an *ideal vocabulary* with a ground-truth target label set or with few open words (Wu et al. 2023; Xu et al. 2023; Karazija et al. 2023).

Zero-Shot Transfer/Unsupervised Fine-tuning of VLMs. Both *Zero-Shot Transfer* (ZST) and *Unsupervised Fine-tuning* (UF) assume no annotation of target datasets. ZST (Radford et al. 2021; Ren et al. 2022) directly uses the pre-trained VLMs for zero-shot prediction without updating models, *e.g.*, SCD (Han et al. 2023) iteratively refines CLIP inference results with a heuristic algorithm with a WordNet vocabulary (Miller 1995). More related to us, UF further transductively adapts pre-trained models with task-specific training, *e.g.* adapting VLMs with self-training or prompt tuning (Li, Savarese, and Hoi 2022; Kahana, Cohen, and Hoshen 2022; Shin, Albanie, and Xie 2023). However, existing methods assume the known ground-truth target label set or label distribution (Kahana, Cohen, and Hoshen 2022; Li, Savarese, and Hoi 2022). In this paper, we aim to alleviate the dependence on such assumptions and propose a new setting, RZSC.

Discussion on Zero-Shot Settings. Here, we summarize the main differences between our RZSC setting and others in Table 1. Previous related settings adopt restrictive assumptions including an ideal vocabulary, the target label distribution, and labeled known classes. Unlike related settings with restrictive assumptions such as an ideal vocabulary, the target label distribution, and known labeled classes, our RZSC seeks to learn to categorize an unlabeled dataset with a huge vocabulary with over 20K classes. An expanded huge vocabulary presents significant challenges for RZSC problem, as evidenced by the consistent and dramatic CLIP performance drop (in Fig. 1 a) on all datasets when the vocabulary scales up. The primary challenge arises from increased open words, complicating fine-grained category discrimination for pre-trained VLMs. As displayed in Fig. 1 b, the averaged cosine similarity between a query text embedding and its 3-nearest text neighbors grows with the vocabulary size. We include more related works in our appendix B.

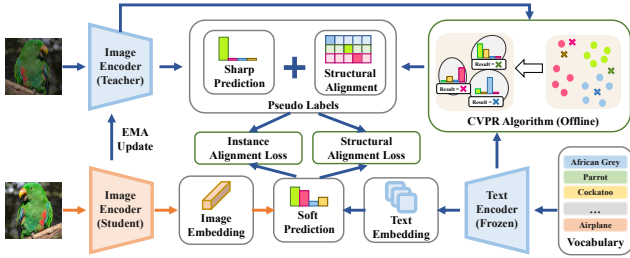


Figure 2: **Illustration of our Self Structural Semantic Alignment (S³A) framework**, which fine-tunes pre-trained CLIP encoder with a teacher-student architecture. The teacher is updated by the student with the exponentially moving average technique. The student is guided by on-the-fly one-hot instance alignment predicted by the teacher; meanwhile, it self-learns the structural semantic alignment labels generated by our per-epoch CVPR algorithm on all teacher image embeddings.

Methodology

Problem: Realistic Zero-Shot Classification

Existing methods that adapt pre-trained VLMs to unseen data usually hinge on specific knowledge of target datasets, such as prior distributions or an ideal vocabulary. These conditions are often challenging to fulfill in real-world environments. In this paper, we explore a more practical task, Realistic Zero-Shot Classification, abbreviated as RZSC.

RZSC is formally defined as follows: Let us consider an unlabeled dataset $\mathcal{D}_u = \{(\mathbf{x}_i, y_i)\}_{i=1}^N \subset \mathcal{X} \times \mathcal{Y}$ with N instances defined on category set \mathcal{Y} , and a pre-trained VLM such as CLIP, equipped with image and text encoders f_I and f_T , respectively. Then, we assume no information of \mathcal{Y} and instead with a comprehensive vocabulary that contains more than 20,000 distinct category names, *i.e.*, $|\mathcal{Y}| \ll |\mathcal{W}|$. We build our vocabulary from all visual categories from ImageNet1K (Deng et al. 2009) and ImageNet21K (Ridnik et al. 2021) datasets since they are annotated with expert taxonomic knowledge (Miller 1995) and encompasses most commonly-seen visual categories in the real world. The goal of the RZSC task is to refine the f_I to predict the correct category:

$$\hat{y}_i = \arg \max_{w_j \in \mathcal{W}} \mathbf{z}_i \cdot \mathbf{h}_j, \quad (1)$$

where $\mathbf{z}_i = f_I(\mathbf{x}_i)$ denotes the image embedding while text embedding $\mathbf{h}_j = f_T(w_j)$ are obtained with a text prompt, *e.g.*, “a photo of [CLS]”, and the category name w_j . Here, \cdot denotes the cosine similarity.

Overview: Self Structural Semantic Alignment

RZSC presents a more formidable challenge than previous tasks, primarily owing to the absence of label information and an increased vocabulary size. As illustrated in part (a) of Fig. 1, the performance of CLIP declines sharply as the vocabulary size increases. This decline can be attributed to the introduction of open redundant words as hard negative samples, which creates noise and confuses the CLIP model, hindering its ability to accurately identify pseudo labels.

It motivates us to propose the Self Structural Semantic Alignment (S³A) framework, aiming at discovering the structural semantics through interactive self-alignment between visual images and textual vocabulary. As shown in Fig. 2, S³A deploys a Cluster-Vote-Prompt-Realign (CVPR) algorithm to explore structural semantics as pseudo labels, and utilizes a self-training procedure to iteratively refine both models and pseudo supervision. Our CVPR algorithm and the self-training procedure mutually enhance each other: as training progresses in adapting representations, the teacher model can provide increasingly reliable pseudo alignments in subsequent iterations of the CVPR algorithm. Concurrently, the CVPR algorithm contributes structural semantics as part of the supervisory signal for self-training. We elaborate on all components in the sections that follow.

Cluster-Vote-Prompt-Realign

The Cluster-Vote-Prompt-Realign (CVPR) algorithm lies at the heart of the S³A framework, representing an innovative approach to uncovering structural semantics in data. As illustrated in Fig. 3, the CVPR algorithm consists of four key stages, each contributing to the alignment and identification of structural relationships between visual images and textual vocabulary, including discovering semantic clusters, voting category names on large vocabulary, prompting LLM to discriminate the nuanced candidates, and refine the cluster-vocabulary alignment. Each step is explained in detail in the subsequent paragraphs. Below we delineate these stages and their functions within the algorithm.

Clustering. Based on existing evidence (Radford et al. 2021) and our observation, the pre-trained CLIP excels at grouping instances with the same or similar semantic labels in the image embedding space. We thus produce the pseudo supervision by semantic clustering and aligning the clusters with vocabulary. Specifically, given image embeddings \mathbf{z}_i in \mathcal{D}_u , we apply KMeans (Arthur and Vassilvitskii 2007) to obtain the K clusters, $\Gamma = \{\Gamma_k\}_{k=1}^K$, where Γ_k denotes the k -th set of image embeddings.

Voting. Given the semantic cluster results Γ , we compute a vocabulary voting distribution matrix $M \in \mathbf{R}^{K \times |\mathcal{W}|}$, where $M_{k,j}$ represents the normalized frequency of the prototype of category w_j being the nearest neighbor to all instances in the k -th cluster. Specifically, it is computed as

$$M_{k,j} = \frac{1}{K|\Gamma_k|} \sum_{\mathbf{z} \in \Gamma_k} \mathbb{I}(w_j = \arg \max_w \mathbf{z} \cdot \mathbf{h}) \quad (2)$$

where \mathbb{I} is an indicator function, and $|\Gamma_k|$ denotes the size of the k -th cluster. Rather than naively assigning each cluster the argmax from the vocabulary, we assign the top- m frequent words to each cluster as potential candidates which are treated equally. It indicates that for each row $M_k = (M_{k,j})_{j=1}^{|\mathcal{W}|}$, we maintain the highest m elements as 1 and others as 0.

Nonetheless, the initial clustering and voting may introduce noise, leading to low-quality pseudo-labels. To mitigate this issue, we iteratively refine the previous clusters based on the current voting outcomes. In particular, we utilize the Hungarian matching (Kuhn 1955) for textual em-

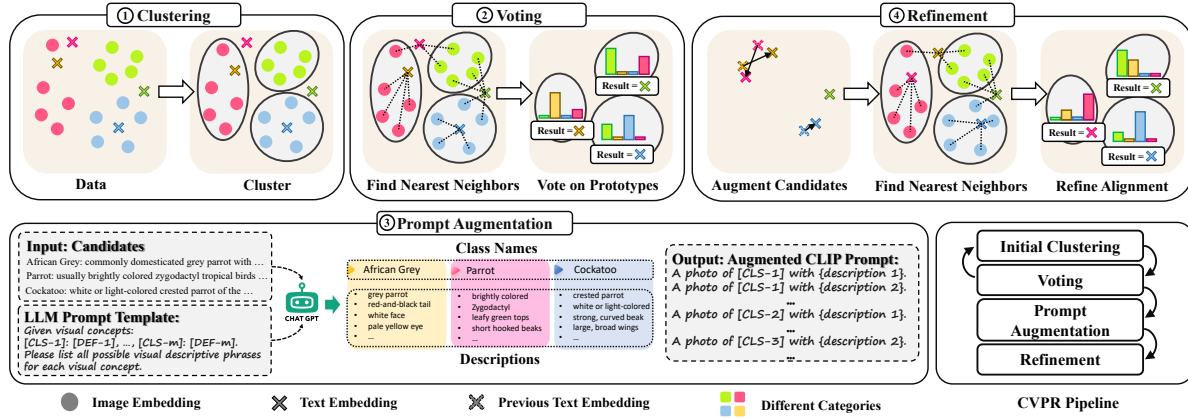


Figure 3: **An illustrative toy example for our CVPR algorithm**, which comprises four steps: (1) We clustering all image embeddings; (2) We conduct 1-nearest neighbor voting on all text prototypes of the large vocabulary for each cluster. Since the results of the naive assignment in this step are susceptible to the noise of text embeddings, we generate cluster-wise candidate categories instead. (3) We augment CLIP text prompts with visual discriminative descriptions from the large language model to discern nuanced candidates. (4) with augmented prompts, the cluster-vocabulary alignment is calibrated and refined.

beddings and clusters to establish a prototype for each cluster. Subsequently, we reassigned the image embeddings, using these prototypes as the updated cluster centers (Han et al. 2023). Additional details are provided in our appendix C.

Prompting. Through our empirical studies, we observed that CLIP’s representation struggles to differentiate nuanced candidates effectively. This observation spurred our efforts to refine the embeddings of textual candidates. We speculate that the challenge in distinguishing fine-grained options arises from the presence of noisy or imprecise image-caption alignments during CLIP’s pre-training.

To address this, our approach is to enhance the basic CLIP prompts by accentuating the subtle semantic differences. We do this by integrating auxiliary textual knowledge drawn from a large language model, renowned for its expertise in knowledge retrieval (Dale 2021; Yang et al. 2021).

To achieve this, we feed m candidate category words from the k -th cluster into the LLM prompt template, each accompanied by their specific definition. Furthermore, to extract nuanced visual attributes from the LLM, we append an instruction to the main prompt, directing the model to emphasize and describe these specific attributes. Our prompt template is structured as follows:

Prompt: Given visual concepts: [CLS-1] : [DEF-1], ..., [CLS- m] : [DEF- m].

Instruction: Goal: to discriminate these visual concepts in a photo. Please list all possible visual descriptive phrases for each visual concept.

In this template, [CLS] represents the concept name, and [DEF] stands for its definition from WordNet (Miller 1995). The LLM then generates a roster of distinctive attributes for each category, such as ‘red-and-black tail’. Each (category, attribute) pair is filled into an ensemble of CLIP prompts, e.g., “A photo of a {category} with {attribute}.”, and forms an augmented text em-

bedding. This forms an enhanced text embedding. For practicality and clarity, and to sidestep ambiguity arising from the polysemy phenomenon, we utilize all synsets and their definitions from WordNet (Miller 1995) for a single category as the input visual concepts for the LLM prompt.

Re-alignment. During the re-alignment phase, our goal is to enhance the structural semantic alignments outlined in Eq. 2. We achieve this by re-establishing alignments between image clusters and the enriched text embeddings from the earlier step. The refined structural semantic alignment, $\tilde{M} \in \mathbf{R}^{K \times |\mathcal{W}|}$, is derived by casting votes on all augmented text embeddings produced in the prompting stage.

To be precise, the alignment relationship between the k -th cluster and word w_j is determined by the normalized sum of occasions where the category w_j ranks within the top-3 closest matches for all image embeddings $\mathbf{z} \in \Gamma_k$, w.r.t. all augmented text embeddings \mathcal{A}_k . The process can be described by the equation:

$$\tilde{M}_{k,j} = \frac{1}{3K|\Gamma_k|} \sum_{\mathbf{z} \in \Gamma_k} \mathbb{I}(w_j \in \arg \text{top3}(\mathbf{z}, \mathcal{A}_k)) \quad (3)$$

where, top3 identifies the three closest words to the query image embedding \mathbf{z} , determined using cosine distance. Meanwhile, \arg extracts the category name linked with the enriched text embedding. In the matrix $\tilde{M}_{k,j}$, each row signifies the voting probability of the top-3 vocabulary terms for the k -th cluster. To establish a clear relationship between clusters and words, we employ the maximum Hungarian matching technique (Kuhn 1955) on a bipartite graph, using the weight matrix \tilde{M} . This approach ensures that no category is linked with multiple clusters. Consequently, every cluster is paired with a unique pseudo category label.

Self Training with Semantic Alignment

In this section, we present our S³A self-training method, as depicted in Fig. 2. The self-training process leverages both

instance-wise and structural alignment pseudo labels which are produced by using an exponentially moving averaged (EMA) teacher model. Throughout this procedure, we refine the CLIP image encoder to improve its representational capabilities, and fix the text encoder instead.

Structural Semantic Alignment. To incorporate the structural semantic alignments, computed by our CVPR algorithm, into online self-training, one challenge needs to be addressed. It is critical to determine the uniform interval for computing pseudo labels from our CVPR across all datasets. For quality pseudo-labels with our CVPR algorithm, using consistent model embeddings is crucial, but collecting them is computationally costly, and determining the optimal execution interval across datasets is challenging. To mitigate these issues, we introduce a slowly updated Exponentially Moving Average (EMA) teacher model. This model executes the CVPR algorithm once per epoch to yield stable and reliable pseudo labels, which then guide the self-training of a student model (Grill et al. 2020).

We define the structural semantic alignment loss as the cross-entropy between the predictions of the student model and the pseudo labels generated by the teacher model. Formally, this loss for the i -th instance can be expressed as:

$$L_{str}(\mathbf{x}_i) = -\hat{\mathbf{p}}_T^T(i) \log \mathbf{p}_S(\mathbf{x}_i). \quad (4)$$

In this equation, $\hat{\mathbf{p}}_T(i)$ represents the one-hot pseudo label for the i -th instance, which is inferred from the teacher model during the last epoch. On the other hand, \mathbf{p}_S denotes the softmax prediction of the student model over the entire vocabulary, computed for the input \mathbf{x}_i .

Individual Semantic Alignment. In addition to the structural semantic alignment loss, we also guide our model with instance-wise pseudo alignments, which are generated on-the-fly by the EMA teacher model. Without this guidance, our model would likely converge to suboptimal solutions rapidly. We formulate the individual semantic alignment loss for the i -th instance as follows:

$$L_{in}(\mathbf{x}_i) = -\mathbb{I}(\tilde{\mathbf{p}}_T(\mathbf{x}_i) > \tau) \tilde{\mathbf{p}}_T^T(\mathbf{x}_i) \log \mathbf{p}_S(\mathbf{x}_i). \quad (5)$$

In this equation, $\tilde{\mathbf{p}}_T$ represents the one-hot sharpened pseudo label produced by the teacher model at each iteration. The symbol τ denotes a confidence threshold, which ensures that the loss is computed only for samples for which the teacher model has a high level of confidence.

To strike a balance between the structural and instance alignment losses, we introduce a weighted combination of both. This approach not only helps the model escape from rapid convergence to local optima but also refines the representations used for future pseudo alignment generation. Consequently, our total loss function for the i -th instance is formulated as:

$$L(\mathbf{x}_i) = L_{str}(\mathbf{x}_i) + \gamma L_{in}(\mathbf{x}_i). \quad (6)$$

Here, γ represents a balancing factor that weights the contribution of the instance alignment loss relative to the structural alignment loss. This total loss is computed at each iteration, based on our CVPR algorithm which is executed once per epoch on the teacher model.

We present entire details of our **S³A** training algorithm together with implementation details in our appendix C.

Experiments

Evaluation

Datasets. We evaluate **S³A** on two generic and five fine-grained benchmarks, *i.e.*, the generic benchmarks of sampled ImageNet-100 (IN100) and ImageNet-1K (IN1K) (Deng et al. 2009), and fine-grained benchmarks of StanfordDogs (SDogs) (Khosla et al. 2011), Living17 (LV17), Nonliving26 (NL26), Entity13 (ET13), and Entity30 (ET30) in BREEDS (Santurkar, Tsipras, and Madry 2020)). Furthermore, we evaluate our **S³A** on three benchmarks for the out-of-vocabulary evaluation (containing categories out of our vocabulary), *i.e.*, Oxford-IIIT Pet (Pet) (Parkhi et al. 2012), CIFAR100 (Krizhevsky, Hinton et al. 2009), and Caltech101(Caltech) (Fei-Fei, Fergus, and Perona 2004). The profile of datasets is listed in our appendix A.

Metrics We adopt the top-1 classification accuracy and clustering accuracy (following SCD (Han et al. 2023) and defined below) for the evaluation.

$$ACC_{clu} = \frac{1}{N} \sum_{i=0}^N \max_{\rho} \mathbb{I}(y_i = \rho(\hat{y}_i)), \quad (7)$$

where ρ is a permutation assignment of cluster indices. y_i and \hat{y}_i are ground-truth predicted categories. Meanwhile, we adopt Intersection-over-Union (IoU) score as an auxiliary metric in ablations to inspect the overlap between our predictions \mathcal{Y}_{pred} and the ground-truth label set \mathcal{Y}_{gt} , *i.e.*, $\frac{|\mathcal{Y}_{pred} \cap \mathcal{Y}_{gt}|}{|\mathcal{Y}_{pred} \cup \mathcal{Y}_{gt}|}$. In the out-of-vocabulary experiments, some class names cannot be found in the vocabulary. Thus, we instead apply a soft accuracy score, defined as the similarity between the predicted word (in vocabulary) and the ground truth label. Inspired by BertScore (Zhang et al. 2019), we adopt a language model, Sentence-Bert (Reimers and Gurevych 2019), to calculate the similarity.

Baselines RZSC is a new setting in which few baselines are ready-to-use. Thus, we evaluate the baseline methods by reproducing them with officially released codes in our setting. Specifically, we consider CLIP as the naive baseline, and two state-of-the-art methods in ZST and UF, *i.e.*, SCD (Han et al. 2023) and MUST (Li, Savarese, and Hoi 2022). In summary, the following baselines are included for performance comparisons:

- **DINO+KMeans** (Caron et al. 2021): DINO is a contrastive self-supervised learning method. We include it here for clustering quality comparisons. We report only its clustering accuracy as it cannot classify.
- **CLIP** (Radford et al. 2021): a large-scale VLM pre-trained with massive image-caption pairs conducts zero-shot prediction given our vocabulary.
- **CLIP (Group)** (Radford et al. 2021): We sequentially conduct clustering, voting, and Hungarian matching on CLIP image embeddings for structural zero-shot transfer, using **S³A** vocabulary.

Methods	SDogs	IN100	IN1K	LV17	NL26	ET13	ET30	Avg
CLIP (Ideal)	57.59/58.07	84.67/84.90	65.38/65.53	75.24/75.53	80.03/80.05	78.43/78.50	77.99/78.03	74.19/74.37
DINO+KMeans	-/45.99	-/75.16	-/55.27	-/72.52	-/62.81	-/67.37	-/64.69	-/63.40
CLIP	53.43/55.43	29.39/38.54	32.21/39.77	37.31/47.24	33.35/38.96	30.09/40.00	31.23/39.90	35.29/42.83
CLIP (Group)	19.37/55.92	40.62/77.68	26.41/56.92	38.33/68.81	41.09/70.51	32.85/71.08	36.36/70.78	33.57/67.38
MUST	57.20/60.61	33.37/52.56	28.97/37.00	31.71/49.35	35.30/48.68	38.46/58.25	33.41/47.08	36.92/50.50
SCD	52.63/55.93	48.89/77.39	37.06/57.00	43.33/68.81	52.18/71.84	40.46/71.25	46.29/70.89	45.83/67.59
S³A (Our)	58.94/62.19	52.08/82.76	42.43/63.15	48.34/75.57	56.20/75.97	45.21/76.92	50.41/76.14	50.51/73.24

Table 2: **Transductive evaluation on seven benchmarks.** Top-1 classification accuracy scores (left of '/') and clustering accuracy scores (right of '/') are reported in percentage. We highlight the highest scores except for the upper bound.

#Row	Prompt	S.T.	L_{str}	ImageNet-100		Living17	
				Acc	Cluster	Acc	Cluster
1	✗	✗	✗	48.89	77.39	43.33	68.81
2	✓	✗	✗	51.81	79.38	44.60	68.69
3	✗	✓	✗	46.23	81.49	46.28	74.60
4	✗	✓	✓	49.00	82.08	46.55	73.04
5	✓	✓	✓	52.08	82.76	48.34	75.57

Table 3: **Top-1 accuracy and Clustering results for our method ablations on ImageNet-100 and BREEDS-Living17.** We conduct ablations on our discriminative prompt augmentation (Prompt), self-training stage (S.T.), and structural semantic alignment loss (L_{str}).

- **CLIP (Ideal)** (Radford et al. 2021): it denotes zero-shot transfer with pre-trained CLIP but given an ideal vocabulary, showcasing the upper bound performance of CLIP representation.
- **MUST** (Li, Savarese, and Hoi 2022): it is an unsupervised ZSC method leveraging instance-wise unsupervised self-training jointly with self-supervised masked-image prediction. We adapt it with our huge vocabulary.
- **SCD** (Han et al. 2023): it is an unsupervised/semi-supervised zero-shot transfer method with WordNet vocabulary. Its iterative algorithm aligns each cluster with one category name. We adapt it with our **S³A** vocabulary. During the inference, we classify images with K category prototypes discovered at the training phase.

Main Results

To validate the effectiveness of our proposed method, **S³A**, we conducted an extensive evaluation under the Real Zero-Shot Classification (RZSC) setting. We compared **S³A** with various baselines on both fine-grained and generic datasets. The results, including classification and clustering accuracies, are reported in Table 2.

Our method, **S³A**, consistently achieves SOTA results, outperforming CLIP by a substantial margin—specifically, over 15% improvement in classification accuracy. Furthermore, **S³A** notably excels over our adapted SOTA baselines, with improvements of nearly 5% in top-1 accuracy and 6% in clustering accuracy. Impressively, it even surpasses CLIP with an ideal vocabulary on the Stanford Dogs dataset. De-

spite CLIP (Group) being augmented with the same clustering information as **S³A**, it encounters significant alignment issues when working with large vocabularies under low-quality clustering, as seen in ImageNet-1K and Stanford Dogs. We posit this superior performance of **S³A** may be attributed to its capacity to dynamically calibrate noisy clustering during the self-learning process. It is noteworthy that the existing SOTA in unsupervised zero-shot classification, MUST, at times fails to improve upon the naive CLIP baseline when using our realistic vocabulary. This underlines the suboptimality of naive self-training methods for RZSC.

Ablations and Analysis

Method Ablations. To validate the contribution of each component of our **S³A**, we conduct method ablation experiments on one generic and fine-grained dataset, *i.e.*, ImageNet-100 and LV17. We present the results in Table 3. The last row represents our full method. When we only keep the initial iterative clustering in our CVPR (the 1st row), our method is equivalent to SCD (Han et al. 2023). The 2nd row denotes our CVPR without all self-training-related components; while, the 3rd row conducts self-training only with instance-wise semantic alignment, similar to MUST (Li, Savarese, and Hoi 2022). The 4th row indicates our **S³A** without LLM knowledge guidance. Based on the results, we can conclude that: (1) Comparing Row 4 & 5, although the clustering quality remains comparable without our discriminative prompt augmentation, the semantic alignment degrades witnessed by the drop in the top-1 accuracy. (2) Comparing Row 1, 2 & 3, self-training dominates the contribution in representation adaptation, witnessed by the cluster performance boosts. (3) Comparing Rows 3 & 4, we observe that the structural alignment loss yields greater improvements on generic datasets, while its effect is less pronounced on fine-grained datasets. This observation is consistent with our expectations, as Hungarian matching proves to be more challenging for fine-grained tasks, due to the potential confusion between closely related categories. In summary, all components of our **S³A** enhance the performance.

Performance on Estimated K . The clustering algorithm requires the number of classes K . In Table 2, we used the ground truth K . In addition, we also offer an iterative algorithm using pre-trained CLIP to enable the data itself to determine an appropriate K , based on the semantic structure of data represented by CLIP (Ouldoughi, Kuo, and Kira 2023;

Methods	LV17 (73)	NL26 (101)	ET13 (252)	ET30 (206)
DINO+KMeans	-72.68	-62.93	-67.41	-63.22
CLIP	37.31/47.24	33.35/38.96	30.09/40.00	31.23/39.90
MUST	31.71/49.35	35.30/48.68	38.46/58.25	33.41/47.08
SCD	40.70/69.17	52.63/70.21	40.12/71.37	45.03/69.14
S³A (Est-K)	49.83/76.23	57.10/75.66	45.54/77.23	47.86/72.75
S³A (GT-K)	48.34/75.57	56.20/75.97	45.21/76.92	50.41/76.14

Table 4: **Transductive evaluation on four fine-grained benchmarks with estimated cluster numbers (Acc/Cluster).** The estimated number is behind the dataset title.

Methods	Caltech (0.34)	CIFAR100 (0.12)	Pet (0.62)
CLIP (Ideal)	91.25/90.96	81.54/81.12	90.87/92.39
CLIP	50.59/49.66	41.62/41.65	55.60/57.96
MUST	51.20/50.80	42.93/42.96	58.32/55.83
SCD	54.08/54.46	42.62/41.64	58.57/57.58
S³A (Our)	55.29/55.55	46.10/46.40	59.00/60.57

Table 5: **Tranductive and inductive evaluation on out-of-vocabulary benchmarks (Train Acc/Test Acc).** The out-of-vocabulary ratios for each dataset are provided alongside their respective names. Performance is reported by cosine similarity of generic pre-trained Sentence-BERT, upscaled by one hundred.

Han et al. 2023), where the detailed algorithm is shown in the appendix C. We present our experimental results on the estimated K in Table 4 on four fine-grained datasets. The estimated K are listed beside the dataset title, which is close to the ground-truth values. We show that the estimated K can also bring comparable results with ground truth ones. Beyond this experiment, we also perform ablation studies to assess the impact of various estimation error scales on K . Detailed results and discussions are in our appendix D.

On Out-Of-Vocabulary (OOV) Scenarios. Considering the scenarios in which target datasets have category names out of our **S³A** vocabulary, we further conduct an out-of-vocabulary evaluation on three benchmarks, *i.e.*, Caltech101 (Fei-Fei, Fergus, and Perona 2004), CIFAR100 (Krizhevsky, Hinton et al. 2009), and Oxford-IIIT Pet (Parkhi et al. 2012). The out-of-vocabulary ratios of datasets and results are presented in Table 5. We can conclude that **S³A** still achieves SOTA performance in this challenging setup on both inductive and transductive evaluation.

On Effectiveness of S³A Prompt Augmentation. In this ablation experiment, we analyze the effect of the proposed LLM-guided discriminative prompt augmentation in our CVPR algorithm. We compare with four augmentation setups in Table 6: (1) using WordNet definition for augmentation (5th row); (2) reduce prompt semantic discriminativeness by requesting visual attributes for only a single category name in each LLM prompt (6th row); (3) our prompt augmentation guided by ChatGPT (7th row); (4) our prompt augmentation guided by GPT-4. Besides, we also compare with a recent SOTA, CHiLS (Novack et al. 2023), in prompt augmentation for zero-shot prediction. We

#Row	Methods	IN1K	ET13	ET30
1	CLIP (Ideal)	65.38/96.58	78.43/99.61	77.99/99.58
2	CLIP	32.21/ 96.49	30.09/ 97.31	31.23/ 95.83
3	SCD	37.06/35.09	40.46/32.31	46.29/39.94
4	CHiLS*	36.23/34.46	41.13/33.33	46.09/39.94
5	Our (WordNet)	18.69/18.42	21.82/16.85	20.38/15.94
6	Our (Single)	37.40/35.74	41.13/33.00	47.09/40.76
7	Our (ChatGPT)	37.69/36.11	42.65/36.84	47.43/41.18
8	Our (GPT-4)	37.95 /36.48	44.98 /37.56	48.37 /42.01

Table 6: **Ablations on prompt augmentation techniques.** Performance is reported by cosine similarity of generic pre-trained Sentence-BERT, upscaled by one hundred. a/b denotes the results of Acc/IoU.

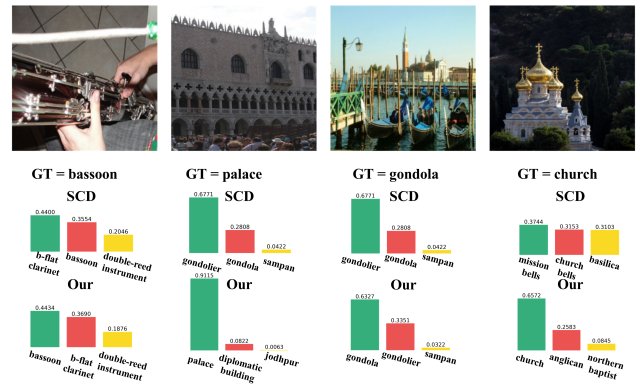


Figure 4: **Qualitative results in IN100 without finetuning (SCD (Han et al. 2023) and our CVPR).**

use their prompt to generate ten subcategories for each class. We can draw the following conclusions: first, semantic distinctiveness in prompts aids fine-grained differentiation; second, incorporating WordNet linguistic knowledge may hinder performance; third, our approach outperforms CHiLS, making it preferable for RZSC tasks; fourth, CLIP’s focus on instance-wise alignment leads to low ACC but high IoU; finally, our method benefits from advanced LLMs.

Qualitative Examples We present qualitative examples from IN100 in Fig. 4 to illustrate the superiority of our semantic structural alignment. The results demonstrate that our offline CVPR algorithm can effectively correct category misrecognitions and precisely focus on salient categories.

Conclusion

In this work, we have tackled the challenging task of Realistic Zero-Shot Classification, without assuming partial source supervision or ideal vocabularies. We have proposed the Self Structural Semantic Alignment (**S³A**) framework, anchored by the innovative Cluster-Vote-Prompt-Realign (CVPR) algorithm for structural semantic mining and a self-training process for iterative semantic alignment. This CVPR algorithm effectively employs unlabeled data to generate structural semantic information, enabling the model to further self-learn and continuously refine its understanding. Our ex-

periments clearly demonstrate the potency of S³A, achieving a significant accuracy improvement relative to baseline methods on various generic and fine-grained benchmarks.

References

Akata, Z.; Perronnin, F.; Harchaoui, Z.; and Schmid, C. 2015. Label-embedding for image classification. *IEEE transactions on pattern analysis and machine intelligence*, 38(7): 1425–1438.

Arthur, D.; and Vassilvitskii, S. 2007. K-means++ the advantages of careful seeding. In *Proceedings of the eighteenth annual ACM-SIAM symposium on Discrete algorithms*, 1027–1035.

Bao, H.; Dong, L.; Piao, S.; and Wei, F. 2021. Beit: Bert pre-training of image transformers. *arXiv preprint arXiv:2106.08254*.

Cappallo, S.; Mensink, T.; and Snoek, C. G. 2016. Video stream retrieval of unseen queries using semantic memory. *arXiv preprint arXiv:1612.06753*.

Caron, M.; Touvron, H.; Misra, I.; Jégou, H.; Mairal, J.; Bojanowski, P.; and Joulin, A. 2021. Emerging properties in self-supervised vision transformers. In *Proceedings of the IEEE/CVF international conference on computer vision*, 9650–9660.

Cubuk, E. D.; Zoph, B.; Shlens, J.; and Le, Q. V. 2020. Randaugment: Practical automated data augmentation with a reduced search space. In *Proceedings of the IEEE/CVF conference on computer vision and pattern recognition workshops*, 702–703.

Dale, R. 2021. GPT-3: What’s it good for? *Natural Language Engineering*, 27(1): 113–118.

Deng, J.; Dong, W.; Socher, R.; Li, L.-J.; Li, K.; and Fei-Fei, L. 2009. Imagenet: A large-scale hierarchical image database. In *2009 IEEE conference on computer vision and pattern recognition*, 248–255. Ieee.

Dosovitskiy, A.; Beyer, L.; Kolesnikov, A.; Weissenborn, D.; Zhai, X.; Unterthiner, T.; Dehghani, M.; Minderer, M.; Heigold, G.; Gelly, S.; et al. 2020. An image is worth 16x16 words: Transformers for image recognition at scale. *arXiv preprint arXiv:2010.11929*.

Fei-Fei, L.; Fergus, R.; and Perona, P. 2004. Learning Generative Visual Models from Few Training Examples: An Incremental Bayesian Approach Tested on 101 Object Categories. *2004 Conference on Computer Vision and Pattern Recognition Workshop*, 178–178.

Gao, P.; Geng, S.; Zhang, R.; Ma, T.; Fang, R.; Zhang, Y.; Li, H.; and Qiao, Y. 2021. Clip-adapter: Better vision-language models with feature adapters. *arXiv preprint arXiv:2110.04544*.

Ghiasi, G.; Gu, X.; Cui, Y.; and Lin, T.-Y. 2021. Open-vocabulary image segmentation. *arXiv preprint arXiv:2112.12143*.

Grill, J.-B.; Strub, F.; Altché, F.; Tallec, C.; Richemond, P.; Buchatskaya, E.; Doersch, C.; Avila Pires, B.; Guo, Z.; Gheshlaghi Azar, M.; et al. 2020. Bootstrap your own latent: a new approach to self-supervised learning. *Advances in neural information processing systems*, 33: 21271–21284.

Han, K.; Li, Y.; Vaze, S.; Li, J.; and Jia, X. 2023. What’s in a Name? Beyond Class Indices for Image Recognition. *arXiv preprint arXiv:2304.02364*.

Jia, C.; Yang, Y.; Xia, Y.; Chen, Y.-T.; Parekh, Z.; Pham, H.; Le, Q.; Sung, Y.-H.; Li, Z.; and Duerig, T. 2021. Scaling up visual and vision-language representation learning with noisy text supervision. In *International conference on machine learning*, 4904–4916. PMLR.

Kahana, J.; Cohen, N.; and Hoshen, Y. 2022. Improving Zero-Shot Models with Label Distribution Priors. *arXiv preprint arXiv:2212.00784*.

Karazija, L.; Laina, I.; Vedaldi, A.; and Rupprecht, C. 2023. Diffusion Models for Zero-Shot Open-Vocabulary Segmentation. *arXiv preprint arXiv:2306.09316*.

Khosla, A.; Jayadevaprakash, N.; Yao, B.; and Li, F.-F. 2011. Novel dataset for fine-grained image categorization: Stanford dogs. In *Proc. CVPR workshop on fine-grained visual categorization (FGVC)*. Citeseer.

Krizhevsky, A.; Hinton, G.; et al. 2009. Learning multiple layers of features from tiny images.

Krizhevsky, A.; Sutskever, I.; and Hinton, G. E. 2017. Imagenet classification with deep convolutional neural networks. *Communications of the ACM*, 60(6): 84–90.

Kuhn, H. W. 1955. The Hungarian method for the assignment problem. *Naval research logistics quarterly*, 2(1-2): 83–97.

Lampert, C. H.; Nickisch, H.; and Harmeling, S. 2009. Learning to detect unseen object classes by between-class attribute transfer. In *2009 IEEE conference on computer vision and pattern recognition*, 951–958. IEEE.

Lei Ba, J.; Swersky, K.; Fidler, S.; et al. 2015. Predicting deep zero-shot convolutional neural networks using textual descriptions. In *Proceedings of the IEEE international conference on computer vision*, 4247–4255.

Li, D.; Li, J.; Li, H.; Niebles, J. C.; and Hoi, S. C. H. 2021. Align and Prompt: Video-and-Language Pre-training with Entity Prompts. *2022 IEEE/CVF Conference on Computer Vision and Pattern Recognition (CVPR)*, 4943–4953.

Li, J.; Li, D.; Savarese, S.; and Hoi, S. 2023. Blip-2: Bootstrapping language-image pre-training with frozen image encoders and large language models. *arXiv preprint arXiv:2301.12597*.

Li, J.; Li, D.; Xiong, C.; and Hoi, S. 2022. Blip: Bootstrapping language-image pre-training for unified vision-language understanding and generation. In *International Conference on Machine Learning*, 12888–12900. PMLR.

Li, J.; Savarese, S.; and Hoi, S. C. 2022. Masked unsupervised self-training for zero-shot image classification. *arXiv preprint arXiv:2206.02967*.

Lin, Y.; Li, C.; Cao, Y.; Zhang, Z.; Wang, J.; Wang, L.; Liu, Z.; and Hu, H. 2022. A Simple Approach and Benchmark for 21,000-Category Object Detection. In *European Conference on Computer Vision*, 1–18. Springer.

Liu, P.; Yuan, W.; Fu, J.; Jiang, Z.; Hayashi, H.; and Neubig, G. 2023. Pre-train, prompt, and predict: A systematic survey

of prompting methods in natural language processing. *ACM Computing Surveys*, 55(9): 1–35.

Loshchilov, I.; and Hutter, F. 2017. Decoupled weight decay regularization. *arXiv preprint arXiv:1711.05101*.

Miller, G. A. 1995. WordNet: a lexical database for English. *Communications of the ACM*, 38(11): 39–41.

Novack, Z.; McAuley, J.; Lipton, Z. C.; and Garg, S. 2023. Chils: Zero-shot image classification with hierarchical label sets. In *International Conference on Machine Learning*, 26342–26362. PMLR.

Ouldnoughi, R.; Kuo, C.-W.; and Kira, Z. 2023. CLIP-GCD: Simple Language Guided Generalized Category Discovery. *arXiv preprint arXiv:2305.10420*.

Parkhi, O. M.; Vedaldi, A.; Zisserman, A.; and Jawahar, C. V. 2012. Cats and dogs. *2012 IEEE Conference on Computer Vision and Pattern Recognition*, 3498–3505.

Pourpanah, F.; Abdar, M.; Luo, Y.; Zhou, X.; Wang, R.; Lim, C. P.; Wang, X.-Z.; and Wu, Q. J. 2022. A review of generalized zero-shot learning methods. *IEEE transactions on pattern analysis and machine intelligence*.

Pratt, S.; Liu, R.; and Farhadi, A. 2022. What does a platypus look like? Generating customized prompts for zero-shot image classification. *ArXiv*, abs/2209.03320.

Radford, A.; Kim, J. W.; Hallacy, C.; Ramesh, A.; Goh, G.; Agarwal, S.; Sastry, G.; Askell, A.; Mishkin, P.; Clark, J.; et al. 2021. Learning transferable visual models from natural language supervision. In *International conference on machine learning*, 8748–8763. PMLR.

Reimers, N.; and Gurevych, I. 2019. Sentence-bert: Sentence embeddings using siamese bert-networks. *arXiv preprint arXiv:1908.10084*.

Ren, S.; Li, L.; Ren, X.; Zhao, G.; and Sun, X. 2022. Rethinking the Openness of CLIP. *arXiv preprint arXiv:2206.01986*.

Ren, S.; Zhang, A.; Zhu, Y.; Zhang, S.; Zheng, S.; Li, M.; Smola, A.; and Sun, X. 2023. Prompt Pre-Training with Twenty-Thousand Classes for Open-Vocabulary Visual Recognition. *arXiv preprint arXiv:2304.04704*.

Ridnik, T.; Ben-Baruch, E.; Noy, A.; and Zelnik-Manor, L. 2021. Imagenet-21k pretraining for the masses. *arXiv preprint arXiv:2104.10972*.

Rousseeuw, P. J. 1987. Silhouettes: a graphical aid to the interpretation and validation of cluster analysis. *Journal of computational and applied mathematics*, 20: 53–65.

Santurkar, S.; Tsipras, D.; and Madry, A. 2020. Breeds: Benchmarks for subpopulation shift. *arXiv preprint arXiv:2008.04859*.

Sariyildiz, M. B.; Kalantidis, Y.; Larlus, D.; and Alahari, K. 2021. Concept generalization in visual representation learning. In *Proceedings of the IEEE/CVF International Conference on Computer Vision*, 9629–9639.

Shao, Z.; Yu, Z.; Wang, M.; and Yu, J. 2023. Prompting Large Language Models with Answer Heuristics for Knowledge-based Visual Question Answering. *ArXiv*, abs/2303.01903.

Shin, G.; Albanie, S.; and Xie, W. 2023. Zero-shot Unsupervised Transfer Instance Segmentation. In *Proceedings of the IEEE/CVF Conference on Computer Vision and Pattern Recognition*, 4847–4857.

Vaze, S.; Han, K.; Vedaldi, A.; and Zisserman, A. 2022. Generalized Category Discovery. In *Proceedings of the IEEE/CVF Conference on Computer Vision and Pattern Recognition (CVPR)*, 7492–7501.

Wang, W.; Zheng, V. W.; Yu, H.; and Miao, C. 2019. A survey of zero-shot learning: Settings, methods, and applications. *ACM Transactions on Intelligent Systems and Technology (TIST)*, 10(2): 1–37.

Wu, J.; Li, X.; Yuan, S. X. H.; Ding, H.; Yang, Y.; Li, X.; Zhang, J.; Tong, Y.; Jiang, X.; Ghanem, B.; et al. 2023. Towards Open Vocabulary Learning: A Survey. *arXiv preprint arXiv:2306.15880*.

Xu, J.; Liu, S.; Vahdat, A.; Byeon, W.; Wang, X.; and De Mello, S. 2023. Open-vocabulary panoptic segmentation with text-to-image diffusion models. In *Proceedings of the IEEE/CVF Conference on Computer Vision and Pattern Recognition*, 2955–2966.

Yang, Z.; Gan, Z.; Wang, J.; Hu, X.; Lu, Y.; Liu, Z.; and Wang, L. 2021. An Empirical Study of GPT-3 for Few-Shot Knowledge-Based VQA. *ArXiv*, abs/2109.05014.

Zang, Y.; Li, W.; Zhou, K.; Huang, C.; and Loy, C. C. 2022. Open-vocabulary detr with conditional matching. In *Computer Vision–ECCV 2022: 17th European Conference, Tel Aviv, Israel, October 23–27, 2022, Proceedings, Part IX*, 106–122. Springer.

Zhang, J.; Huang, J.; Jin, S.; and Lu, S. 2023. Vision-language models for vision tasks: A survey. *arXiv preprint arXiv:2304.00685*.

Zhang, T.; Kishore, V.; Wu, F.; Weinberger, K. Q.; and Artzi, Y. 2019. BERTscore: Evaluating text generation with bert. *arXiv preprint arXiv:1904.09675*.

Zhou, C.; Loy, C. C.; and Dai, B. 2022. Extract free dense labels from clip. In *European Conference on Computer Vision*, 696–712. Springer.

Zhou, K.; Yang, J.; Loy, C. C.; and Liu, Z. 2022a. Learning to prompt for vision-language models. *International Journal of Computer Vision*, 130(9): 2337–2348.

Zhou, X.; Girdhar, R.; Joulin, A.; Krähenbühl, P.; and Misra, I. 2022b. Detecting twenty-thousand classes using image-level supervision. In *European Conference on Computer Vision*, 350–368. Springer.

Zhou, Z.; Lei, Y.; Zhang, B.; Liu, L.; and Liu, Y. 2023. Zegclip: Towards adapting clip for zero-shot semantic segmentation. In *Proceedings of the IEEE/CVF Conference on Computer Vision and Pattern Recognition*, 11175–11185.

Zhu, X.; Zhang, R.; He, B.; Zeng, Z.; Zhang, S.; and Gao, P. 2022. PointCLIP V2: Adapting CLIP for Powerful 3D Open-world Learning. *ArXiv*, abs/2211.11682.

Towards Realistic Zero-Shot Classification via Self Structural Semantic Alignment – Supplementary Material

A Dataset Profile

We report the details of our benchmarks in our main results in Table S-7. Additionally, we also present the out-of-vocabulary benchmark details in Table S-8.

B Additional Related Work

Prompt Augmentation. Prompt augmentation has proven conducive to multi-modal zero-shot transfer by providing supplementary information in addition to raw category names to better capture the training data distribution (Liu et al. 2023; Radford et al. 2021). The simplest practice is ensembling prompts with handcrafted templates (Radford et al. 2021). Further, driven by the powerful knowledge retrieval capability of emergent LLMs (Dale 2021; Shao et al. 2023), some recent works (Novack et al. 2023; Pratt, Liu, and Farhadi 2022; Zhu et al. 2022) propose to augment text-prompt templates by querying LLM for class-specific semantic information (e.g., attributes) or incorporating dataset-specific domain knowledge. Based on our empirical comparisons, our proposed VTA augmentation is better at distinguishing between fine-grained semantic categories.

Learning with Large Vocabulary. Recently, large vocabulary vision tasks grow popular in the research community. POMP (Ren et al. 2023) proposes to utilize few-shot examples in ImageNet-21K (Ridnik et al. 2021) to enhance the generalization capability of CLIP on downstream tasks/datasets. Detic (Zhou et al. 2022b) proposes to employ massive image-labeled images from ImageNet-21K to tune a detector classifier of over 20K categories for open-vocabulary object detection. Meanwhile, (Lin et al. 2022) also proposes a simple two-stage baseline for the object detection task, which jointly learns from large-vocabulary classification data and small-vocabulary detection. However, their methods are orthogonal to ours, since they treat images from a large number of categories as labeled source data to benefit generalization towards downstream datasets; while our learning goal is to categorize an unseen unlabeled dataset with no supervision.

C S³A Training Algorithm

More Details on CVPR Algorithm

Iterative Clustering. In the clustering step of our CVPR, we incorporate additional iterative clustering steps (Han et al. 2023), which refine the previous cluster results with voting results on textual prototypes. Suppose the clustering partition at t -th step is Γ^t , and its top-1 voting matrix is $M^t \in \mathcal{R}^{K \times |\mathcal{W}|}$, we assign each cluster with a distinct category name by Hungarian matching, *i.e.*, solving maximum-weight bipartite matching between K clusters and $|\mathcal{W}|$ words based on the weight matrix M^t . Formally, this optimization problem of bipartite matching is formu-

lated as:

$$\begin{aligned} \max_A \quad & \text{tr}(M^t A^T) \\ \text{s.t.} \quad & \sum_{j=1}^{|\mathcal{W}|} A_{kj} = 1, \quad \forall k \in \{1, \dots, K\} \\ & \sum_{k=1}^K A_{kj} \leq 1, \quad \forall j \in \{1, \dots, |\mathcal{W}|\} \\ & A_{kj} \in \{0, 1\}, \quad \forall k, j \end{aligned} \quad (8)$$

where $A \in \mathcal{R}^{K \times |\mathcal{W}|}$ is the 0-1 assignment matrix. Here, $A_{k,j} = 1$ denotes the j -th word is assigned to the k -th cluster, and $A_{k,j} = 0$ otherwise. We omit the superscript t for A for notation simplicity.

After A has been resolved, the textual prototypes of K assigned words are considered as common argmax (pseudo) classifiers which cluster all image embeddings into the updated partition Γ^{t+1} . Then, the image clusters Γ^{t+1} follow the same previous process. This iteration terminates until the partition Γ^{t+1} does not change any further.

Estimation of K using CLIP. We propose a simple iterative estimation technique to estimate the class number of an unlabeled dataset based on CLIP image embeddings. GCD (Vaze et al. 2022) utilizes the elbow algorithm to determine the optimal cluster count K by pinpointing the inflection in cluster scores across a predefined K range. This 'elbow' or inflection arises when there is a noticeable deceleration in the reduction of clustering scores. For our clustering metric, we employ the Silhouette score (Rousseeuw 1987). Relying solely on a single-pass elbow algorithm can make the estimated K vulnerable to noise. To address this, our iterative approach consists of three passes: first, we scan the range $[\text{LB}_0, \text{UB}_0]$, then $[\text{LB}_0, S_1]$, and finally $[S_2, \frac{S_2+S_1}{2}]$, each time applying the elbow algorithm. Here, S_1 and S_2 denote the solution of the first and second pass. In practice, we consistently set $\text{LB}_0 = 50$ and $\text{UB}_0 = 2000$ across all datasets, and our experiments show that the iterative method offers improved precision over the single-pass approach (see Table S-9).

Training Algorithm. In this part, we delineate our S³A training algorithm, which is presented in algo. 1. At each training epoch, we first conduct our CVPR algorithm on all extracted image embeddings from the teacher model to obtain the semantic structural alignment labels \hat{Y} (from line 6 to line 18). During the training (from line 19 to line 24), we compute two loss functions: (1) instance semantic alignment loss between one-shot pseudo-label from the teacher model, *i.e.*, the nearest neighbor prediction of each instance on our vocabulary; (2) structural semantic alignment loss between student predictions and our structural pseudo labels \hat{Y} . Finally, the teacher is EMA updated with EMA decay η by student parameters.

Implementation Details of S³A

For our method, we construct our S³A huge taxonomic vocabulary from all distinct class names in ImageNet-

Dataset	StanfordDogs	ImageNet-100	ImageNet-1K	Living17	Nonliving26	Entity13	Entity30
#Train	12K	127K	1M	88K	132K	334K	307K
#Test	8K	5K	50K	3K	5K	13K	12K
#Category	120	100	1000	68	104	260	240

Table S-7: **The profile of seven benchmarks for performance comparisons.** Here, we report the training set size, test set size, and category name.

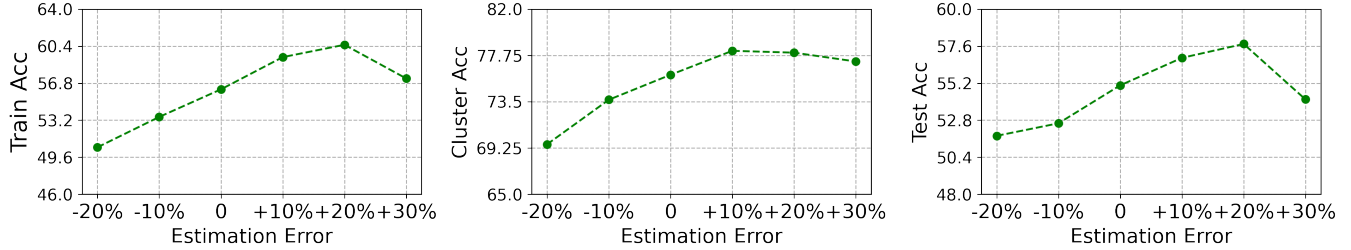


Figure S-5: **Assessing sensitivity to errors in K estimation.** We present results corresponding to different percentages of estimation inaccuracies relative to the true value of K .

Dataset	Caltech101	CIFAR100	Pet
#Train	6K	50K	3K
#Test	1K	10K	3K
#Category	100	100	37
%OOV	34	12	62

Table S-8: **The profile of three benchmarks for out-of-vocabulary evaluation.** Here, we report the training set size, test set size, total category number, and out-of-vocabulary ratio of category names.

Method	LV17	NL26	ET13	ET30
Ground-truth	68	104	260	240
Single-pass	52	87	323	201
Iterative (Our)	73	101	252	206

Table S-9: Different methods to estimate K .

21K (Ridnik et al. 2021) and ImageNet-1K (Krizhevsky, Sutskever, and Hinton 2017) datasets, which is comprehensive enough to cover all common classes in downstream datasets (Sariyildiz et al. 2021; Ridnik et al. 2021). We fix $m = 3$ and $\gamma = 0.25$ across all datasets. The class number K of the target dataset is assumed known unless specified. Considering requesting LLM is time-demanding, we only compute prompting at the first epoch.

We apply strong augmentations for the student, *i.e.*, RandomResizedCrop, RandomFlip, and RandAug (Cubuk et al. 2020), and weak augmentations for the teacher, *i.e.*, Resize, and RandomCrop. We adopt ViT-B/16 (Dosovitskiy et al. 2020) as our CLIP backbone for main evaluation. Following (Li, Savarese, and Hoi 2022), we utilize AdamW (Loshchilov and Hutter 2017) optimizer with a learning rate of $1e^{-5}$, a batch size of 128, and a weight decay of 0.05. The cosine learning rate schedule without warmup

Params	IN/BREEDS	SDogs	Caltech	CIFAR	Pet
Init. EMA	0.999	0.999	0.999	0.999	0.99
EMA Iter.	2000	2000	2000	500	100
τ	0.5	0.5	0.5	0.3	0.7
Epoch	30	30	30	30	60

Table S-10: **Hyperparameters for all benchmarks**, including the initial EMA weight decay value, EMA warmup iterations, confidence parameter τ , and training epoch number.

Methods	IN100	LV17	NL26	ET13	ET30	Avg
CLIP (Ideal)	89.09	80.17	84.38	83.87	82.33	83.77
CLIP	34.82	43.59	36.95	35.62	36.44	37.48
SCD	50.61	54.10	55.23	48.82	49.44	51.64
S^3A -CVPR (Our)	52.51	55.31	56.02	51.31	52.78	53.59

Table S-11: **Transductive evaluation on five benchmarks for backbone ablations.** Top-1 classification accuracy scores are reported in percentage. We highlight the highest scores except for the upper bound. The evaluation is conducted for the CLIP ViT-L/14 backbone.

is adopted. Following (Bao et al. 2021), we also adopt layer-wise learning rate decay of 0.65. Notice that we train for 30K iterations at maximum across all datasets. Besides, we present details on other hyperparameters in Table S-10. Specifically, we linearly warmup the EMA decay parameter from the specified initial EMA value to 0.9998 within specified iterations in Table S-10, following (Li, Savarese, and Hoi 2022). We observe negligible random variances in final results since our S^3A is deterministic and our randomness only comes from the optimizer. For backbone ablations, we increase the initial learning rate to $2e^{-5}$ for ViT-L/14 backbone. During the inference, we adopt the teacher model for inference with the weak data augmentation on our entire

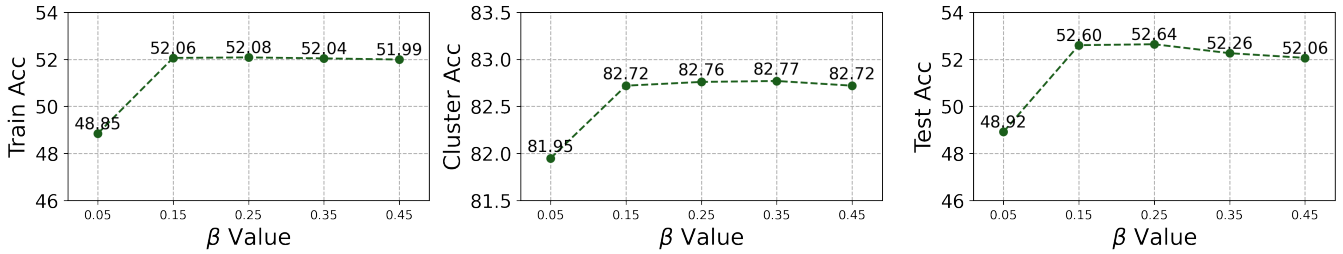


Figure S-6: **Ablation study on the structural semantic alignment loss weight β .** By default, we set $\beta = 0.25$.

Methods	Train Acc	Cluster Acc	Test Acc
CLIP (Ideal)	83.87	83.21	83.20
CLIP (ViT-L/14)	35.62	40.00	33.91
SCD (ViT-L/14)	48.82	76.24	46.91
MUST (ViT-L/14)	43.29	58.25	37.63
S³A (ViT-B/16)	45.21	76.92	45.65
S³A (ViT-L/14)	52.61	81.00	53.32

Table S-12: **Transductive evaluation on BREEDS-ET13 benchmarks for backbone ablations.** We highlight the highest scores except for the upper bound. The evaluation is conducted for the CLIP ViT-L/14 backbone.

Method	SDogs	IN100	ET13	ET30	Pet
BLIP-2	43.49	47.57	54.60	52.96	54.05
BLIP-2 (Group)	45.01	51.65	59.60	58.17	55.12
S³A (Our)	78.45	75.77	70.73	73.86	59.00

Table S-13: **Additional evaluation for comparing with BLIP-2 LMM.** The scores are reported with soft accuracies based on Sentence-BERT similarity.

S³A vocabulary for predictions. All experiments are conducted on a single RTX A6000 GPU.

D Additional Experimental Results

Ablations on Different Backbones. Besides the main results in Table 2, we conduct additional ablations on our offline CVPR algorithm with different CLIP backbones, *i.e.*, ViT-L/14, and report our results in Table S-11. We can observe that, even without self-alignment fine-tuning, our method can considerably surpass our adapted SOTA, *i.e.*, SCD, with nearly 2% in the top-1 accuracy. Moreover, we present our results in Table S-12 on a randomly chosen benchmark, *i.e.*, BREEDS-Entity13, to compare our entire method with other baselines. Further, we conclude that our entire method with self semantic alignment tuning can achieve significant performance advancement with $\sim 4\%$ in classification and $\sim 5\%$ in clustering w.r.t. existing SOTA methods.

Generalization under Inductive Evaluation

Sensitivity to K . To determine the underlying effects of estimation error on K on our **S³A** method, we further assess the

sensitivity of **S³A** performance w.r.t. this estimation error. In Fig. S-5, we showcase results for values of K varying from a decrease of 20% to an increase of 30% from its true value. From our analysis, it is evident that our **S³A** demonstrates substantial resilience to over-fragmentation. However, with an equivalent degree of under-fragmentation error, there is a noticeable performance drop due to a larger increase in the number of instances inaccurately assigned.

Sensitivity to β . We conduct ablation study on the robustness of our **S³A** towards the weight β of the structural semantic alignment loss. The results are presented in Table S-6. In this experiment, we vary the β by 0.1 and 0.2 respectively on both sides. From the findings, we deduce that our **S³A** remains robust with variations in β , unless β is exceedingly small. As β increases, there's a marginal decline in overall performance.

Additional Comparisons with the Large-Multimodal Model (LMM). We further present additional results for comparisons between our **S³A** and the recently proposed powerful LMM, *i.e.*, BLIP-2 (Li et al. 2023), on several benchmarks to showcase the effectiveness of our method. To ensure fair comparisons, we adopt pre-trained BLIP-2 with ViT-B/16 backbone and reproduce the method based on their official code. Our study includes two baselines: (1) In the naive CLIP-2 baseline, we prompt with what is the category name of the object in the photo? c_0 , c_1 , or c_2 ? (where c_0, c_1, c_2 are candidate outputs from SCD (Han et al. 2023)). Here, we treat the generated names as predictions. (2) For the CLIP-2 (Group) baseline, the category name with the highest voting frequency in each cluster (determined using KMeans (Arthur and Vassilvitskii 2007) clustering algorithm) is designated as the prediction for all images within that specific cluster. Given that the LMM output can sometimes fall outside of the expected vocabulary, we utilize soft accuracy scores for the evaluation. The experimental results are displayed in Table S-13. We can conclude that our **S³A** consistently outperforms the powerful BLIP-2 (Li et al. 2023), showcasing its superiority in handling generic, fine-grained, and out-of-vocabulary benchmarks. We speculate that the low performance of BLIP-2 might originate from its unpredictable text generation tendencies evidenced by its occasional production of unrelated words.

Additional Qualitative Examples. We present additional qualitative examples in Fig. S-7 and Fig. S-8 on StanfordDogs and ImageNet-1K to evaluate our **S³A** method

Methods	SDogs	IN100	IN1K	LV17	NL26	ET13	ET30	Avg
CLIP (Ideal)	57.59/	84.67/	65.38/	75.24/	80.03/	78.43/	77.99/	74.19/
CLIP	53.43/	29.39/	32.21/	37.31/	33.35/	30.09/	31.23/	35.29/
CLIP (Group)	19.37/	40.62/	26.41/	38.33/	41.09/	32.85/	36.36/	33.57/
MUST	57.20/58.88	33.37/33.90	28.97/28.72	31.71/31.36	35.30/33.85	38.46/37.57	33.41/33.03	36.92/
SCD	52.63/	48.89/	37.06/	43.33/	52.18/	40.46/	46.29/	45.83/
S³A (Our)	58.94/61.31	52.08/52.64	42.43/42.61	48.34/47.56	56.20/55.06	45.21/45.65	50.41/50.12	50.51/

Table S-14: **Transductive and inductive evaluation on seven benchmarks.** Top-1 classification accuracy scores (left of ‘/’ for the training set and the right for the test set. Accuracy scores are reported in percentage. We highlight the highest scores except for the upper bound.

against other baselines. Our method is robust to both textual fine-grained category names (*e.g.*, trolleybus and shuttle bus) and visual fine-grainedness (*e.g.*, bloodhood and coonhood, ping-pong ball and egg white or gulf ball), which corroborates our **S³A** method has learned more discriminative multi-modal semantic alignments than pre-trained CLIP.

Algorithm 1: S³A Training Algorithm.

Input: Unlabeled Training dataset \mathcal{D}_u , a pre-trained VLM (CLIP) with image encoder $f_I(\cdot|\theta)$ and frozen text encoder $f_T(\cdot)$, large vocabulary \mathcal{W} .

Output: Trained adapted model $f_I(\cdot|\theta)$.

- 1 Initialize teacher encoder $f_{I,T}(\cdot|\theta_S)$ from the student model f_I .
- 2 Precompute textual embeddings $\mathbf{H} = f_T(\mathcal{W})$.
- 3 **for** each epoch $e=1\dots E_1$ **do**
- 4 // Offline: CVPR Algorithm
- 5 $\mathbf{Z} = \phi, \tilde{\mathbf{Y}} = \phi$
- 6 **for** each batch $\mathbf{X} \in \mathcal{D}_u$ **do**
- 7 $\mathbf{Z} = [\mathbf{Z}; f_{I,T}(\mathbf{X})]$ // collect features
- 8 $\tilde{\mathbf{Y}} = [\tilde{\mathbf{Y}}; \text{Nearest}(\mathbf{Z}, \mathbf{H})]$ // collect predictions on vocabulary
- 9 // Iterative Clustering
- 10 $\Gamma^0 = \text{KMeans}(\mathbf{Z}), t = 0$ // initial clustering
- 11 **for** $t \leq \text{max_iter}$ **do**
- 12 Compute M^t from Γ^t with eq. 2 ($m = 1$) and $\tilde{\mathbf{Y}}$. // voting
- 13 Compute cluster-category assignment A from M^t with eq. 8. // Hungarian matching
- 14 Compute new cluster partition Γ^{t+1} by assigning instances \mathbf{Z} to K prototypes from $\{\mathbf{H}_j | \sum_{k=1}^K A_{k,j} = 1\}$.
- 15 $t = t + 1$.
- 16 // Voting
- 17 Let $\Gamma = \Gamma^t$. Compute M from Γ with eq. 2 ($m = 3$) and $\tilde{\mathbf{Y}}$.
- 18 Obtain $\{\mathcal{A}_k\}_{k=1}^K$ with prompt augmentation. // prompting
- 19 Compute \tilde{M} with eq. 3 and obtain structural semantic alignment $\hat{\mathbf{Y}}$ from Hungarian solution A on \tilde{M} . // realigning
- 20 // Online: Self Training with Semantic Alignment
- 21 **for** each batch $(\mathbf{X}, \hat{\mathbf{Y}}) \in \mathcal{D}_u$ **do**
- 22 $\tilde{\mathbf{Y}} = \text{Nearest}(f_{I,T}(\mathbf{X}), \mathbf{H})$. // forward teacher
- 23 $\tilde{\mathbf{Y}}_S = f_I(\mathbf{X})$. // forward student
- 24 // Individual Semantic Alignment Loss
- 25 Compute cross entropy between $\tilde{\mathbf{Y}}_S$ and $\tilde{\mathbf{Y}}$ threshold by confidence τ .
- 26 // Structural Semantic Alignment Loss
- 27 Compute cross entropy between $\tilde{\mathbf{Y}}_S$ and $\hat{\mathbf{Y}}$.
- 28 Update teacher parameters $\theta_S = \eta\theta_S + (1 - \eta)\theta$.
- 29 **return** $f_{I,S}(\cdot|\theta_S)$



GT=	american_staffordshire_terrrier	bloodhound	bluetick	giant_schnauzer	toy_poodle	siberian_husky
CLIP=	staffordshire_bullterrier	coonhound	german_short-haired_pointer	bouvier_des_flandres	miniature_poodle	malamute
SCD=	staffordshire_bullterrier	coonhound	german_short-haired_pointer	bouvier_des_flandres	maltese_dog	malamute
Our=	american_staffordshire_terrrier	bloodhound	bluetick	giant_schnauzer	toy_poodle	siberian_husky



GT=	affenpinscher	kuvasz	giant_schnauzer	chesapeake_bay_retriever	french_bulldog	soft-coated_wheaten_terrrier
CLIP=	terrier	great_pyrenees	scotch_terrier	lapdog	lapdog	tibetan_terrrier
SCD=	norwich_terrrier	great_pyrenees	scotch_terrier	lapdog	lapdog	tibetan_terrrier
Our=	affenpinscher	kuvasz	giant_schnauzer	chesapeake_bay_retriever	french_bulldog	soft-coated_wheaten_terrrier

Figure S-7: **Additional qualitative examples on StanfordDogs dataset.** The ground-truths, and category names predicted by CLIP, SCD, and our S^3A are presented below each image. Green/red texts denote correct/incorrect predictions.



GT=	broccoli	anemone_fish	sea_cucumber	bedlington_terrier	lesser_panda	chiton
CLIP=	broccoli_raab	giant_conch	electric_eel	standard_poodle	red_fox	brook_trout
SCD=	broccoli_raab	chambered_nautilus	slug	standard_poodle	red_fox	northern_pike
Our=	broccoli	anemone_fish	sea_cucumber	bedlington_terrier	lesser_panda	chiton



GT=	harvester	ping_pong_ball	trolleybus	bicycle-built-for-two	coffee_mug	irish_setter
CLIP=	spreader	egg_white	shuttle_bus	safety_bicycle	graduated_cylinder	english_toy_spaniel
SCD=	moldboard_plow	golf_ball	bus	tricycle	graduated_cylinder	toy_dog
Our=	harvester	ping_pong_ball	trolleybus	bicycle-built-for-two	coffee_mug	irish_setter

Figure S-8: **Additional qualitative examples on ImageNet-1K dataset.** The ground-truths, and category names predicted by CLIP, SCD, and our S^3A are presented below each image. Green/red texts denote correct/incorrect predictions.